

Total No. of Pages 100
Copy No. [REDACTED]

REPORT NO. 8

KH-4B SYSTEM CAPABILITY

Evaluation of SO-242 Film
for Use With the KH-4B System

4 AUGUST 1970

Authors: [REDACTED]

[REDACTED]

Declassified and Released by the NRO

In Accordance with E. O. 12958

on NOV 26 1997

Notice of Missing Page(s)

Pages 12, 14, 38, 44, and 46 of the original document apparently were considered parts of oversize pages and were not given separate page numbers.

This page intentionally blank.

CONTENTS

1. Historical Perspective	7
2. Test Description	9
3. Characteristics of SO-242 Film	15
3.1 Physical Structure	15
3.2 Photographic Sensitivity	20
3.3 Resolution Capability	21
4. KH-4B System Analysis With SO-242 Film	29
4.1 Petzval Lens MTF's	29
4.2 SO-242 Dye Layer Isolation	29
4.3 Integral and Analytical Filter Densities	33
4.4 Signal and Noise Perturbations	34
4.5 Lens/Layer MTF Determinations	39
5. Interpretability of Mission 1108 SO-242 Imagery	51
5.1 Resolution Evaluation	51
5.2 Color Evaluation	53
5.3 Specific Subject Evaluation	53
6. Geologic Value of KH-4B System Color Imagery	71
6.1 Producing a Geologic Map	71
6.2 Photogeologic Principles	72
6.3 Northwest Tsaidam Basin Interpretation	78
6.4 Value of Color for Photogeologic Mapping	81
7. Conclusions	93
8. Recommendations	95
Appendices	
A Relative Interpretability Ranking	97
B Exposure Technique for Mission 1108 SO-242 Film	99

FIGURES

2-1	Ground Tracks for Mission 1108 SO-242 Passes Over the United States and Cuba	11
2-2	Ground Tracks for Mission 1108 SO-242 Passes Over Eurasia	13
3-1	Physical Structure of SO-242 and 3404 Films	16
3-2	700× Photomicrographs of Cross Sections of SO-242 and 3404 Films	17
3-3	Reproduction of SO-242 Spectrogram	23
3-4	Spectral Sensitivity of SO-242 Film	23
3-5	Absolute Spectral Sensitivity of SO-242 Film	24
3-6	Normalized Spectral Sensitivities of SO-242 Film Filtered With a Wratten No. 2B and SO-121 Film Filtered With a Wratten No. 2E	25
3-7	Spectral Density of Base-Plus-Stain of SO-242 Film	26
3-8	Dye Absorption Curves for SO-242 Color Film	27
3-9	AIM Curves for SO-242 Film	28
4-1	MTF's for Second and Third Generation Petzval Lenses for the Three Spectral Sensitivities of SO-242 Film	30
4-2	MTF's for Second and Third Generation Petzval Lenses for Three Wavelengths at the Sensitivity Peaks of SO-242 Film	30
4-3	Comparison of Petzval Lens Modulation Transfer Contours	31
4-4	Minor/Major Density Plots for SO-242 Film	35
4-5	Microdensitometer MTF's for Several Spectral Bands	36
4-6	Photographic Noise Characterization in SO-242 Film	37
4-7	450× Enlargements of an Edge Imaged in SO-242 Film Reproduced Through Red, Green, and Blue Filters	41
4-8	Illustration of Steps Involved in Producing an MTF From a Single Edge Trace for the Cyan Dye Layer of SO-242 Film Imaged With a Third Generation Petzval Lens	43
4-9	Lens/Film MTF's Determined From Edge Traces	45
4-10	Yellow Dye Layer IFD and AFD Edge Distributions	47
4-11	Average Petzval Lens/SO-242 Dye Layer MTF's Determined From Edge Traces	48
4-12	Illustration (Not to Scale) of Relative Size of Blur Circles for the Actinic Radiation in Each of the SO-242 Film Layers	49
5-1	10× Enlargement of Snow-Covered Urban and Military Area in the USSR; 3404 Film, Mission 1108-2, Rev D-268, 009 FWD	60
5-2	10× Enlargement of Snow-Covered Urban and Military Area in the USSR; SO-242 Film, Mission 1108-2, Rev D-268, 015 AFT	61
5-3	20× Enlargement of a Town and Pictographs on a Dam in China; 3404 Film, Mission 1108-2, Rev D-264, 002 FWD	62

5-4	20× Enlargement of a Town and Pictographs on a Dam in China; SO-242 Film, Mission 1108-2, Rev D-264, 008 AFT	63
5-5	5× Enlargement of 3404 Film Showing Copper Mines and Processing Facilities in Arizona; Mission 1108-2, Rev D-242, 022 FWD	64
5-6	5× Enlargement of SO-242 Film Showing Copper Mines and Processing Facilities in Arizona; Mission 1108-2, Rev D-242, 027 AFT	65
5-7	10× Enlargements of US Military Airfields for Comparison Purposes	66
5-8	5× Enlargement of the Offshore Islands and Subsurface Features South of Cuba; SO-242 Film, Mission 1108-2, Rev D-273, 022 AFT	67
5-9	Relative Subjective Evaluation of SO-242	68
5-10	Relative Subjective Evaluation of SO-180 and SO-121	69
6-1	Geographic Location and Compilation Limits of the Geologic Mapping and Interpretation of the Tsaidam Basin, Tsinghai Province, China; Reference USAF Jet Navigation Chart JN-24, Scale 1:2,000,000	73
6-2	Geologic Map of the Tsaidam Basin, Tsinghai Province, China; Developed From the SO-242/3404 Coverage of Rev D-249 of Mission 1108-2	74
6-3	3× Enlargement of SO-242 Film Showing an Evaporation Basin and Incised Alluvium in the Chinese Desert Near Lop Nor; Mission 1108-2, Rev D-265, 020 AFT	84
6-4	3× Enlargement of 3404 Film Showing an Evaporation Basin and Incised Alluvium in the Chinese Desert Near Lop Nor; Mission 1108-2, Rev D-265, 014 FWD	85
6-5	Contact Size Illustrations of a Strongly Folded Cretaceous-Tertiary Sedimentary Outcrop in South Central Russia	86
6-6	2× Stereo Pair Showing a Contact Between Jurassic-Cretaceous Sediments and Early Paleozoic Metamorphosis Series; Mission 1108-2, Rev D-249, 018 FWD, 024 AFT	87
6-7	5× Enlargement of 3404 Film Showing Uplifted Anticlinal Fold in the Tsaidam Basin With Detail in Sedimentary Beds; Mission 1108-2, Rev D-249, 021 FWD	88
6-8	5× Enlargement of SO-242 Film Showing Uplifted Anticlinal Fold in the Tsaidam Basin With Colors Present in the Sedimentary Beds; Mission 1108-2, Rev D-249, 027 AFT	89
6-9	10× Enlargement of 3404 Film Showing an Oil Field on a Tightly Folded, Thin Bedded, Tertiary Kansu Anticlinal Structure; Mission 1108-2, Rev D-249, 021 FWD	90
6-10	10× Enlargement of SO-242 Film Showing an Oil Field on a Tightly Folded, Thin Bedded, Tertiary Kansu Anticlinal Structure; Mission 1108-2, Rev D-249, 027 AFT	91

TABLES

3-1 Layer Orientations of the Three Color Films Used in KH-4B Experiments 19
5-1 Comparison of Percentage Absorption of Light Per Meter for Unfiltered
Samples of Sea Water From All Stations Measured After Shaking 57
B-1 No-Snow Exposure Data for Mission 1108 (SO-242 Film) 99

1. HISTORICAL PERSPECTIVE

Mission 1108 was launched on 4 December 1969 and recovered on 21 December during rev 276. As an experiment, 819 feet of SO-242 Aerial Color Film were included as a tag-on to the aft-looking camera film supply. Color coverage was obtained on 13 photographic passes and totalled 213 frames.

Previous missions in this series had acquired color information in various modes on a limited basis. Early KH-4B camera pairs utilized green filter acquisition to complement red filter acquisition on 3404 (black and white) film to provide synthesis of bi-color imagery* with ground handling equipment. Registration difficulties, minimal color cues, and the advent of high resolution color film have since discouraged further use of the bi-color technique on the KH-4B system. Color translation was experimented with on mission 1104-2 by acquiring imagery on SO-180 Infrared Ektachrome Film.† Near-infrared-sensitive layer speed instability, electrostatic discharge fogging, and approximately 30-foot optimum ground resolution performance level have impeded further use of this color approach. An improved version of this material would have a high potential in the KH-4B system. Natural color was acquired with SO-121 Aero Ektachrome film tag-ons to missions 1105-2 and 1106-2 with promising results.‡ There was a film curl anomaly on 1105 and a film separation anomaly on 1106, but capability was demonstrated at a 25-foot optimum ground resolution level.

The improved Aerial Color Film, SO-242, in the system is free of any serious anomalies and has demonstrated both better color discrimination and a 15-foot ground resolution optimum performance level. This document reports the results of the special engineering operations with SO-242 film in the KH-4B system. The objectives established and met for this test were: (1) to obtain improved conventional color photography with the KH-4B system; (2) to demonstrate the in-flight characteristics of SO-242 film in the KH-4B cameras; and (3) to certify operational capability.

*CR-2 Bi-Color Experiment [redacted] (27 Sept 1968). Special Purpose Photographic Techniques for Overhead Reconnaissance. [redacted] (Oct 1969).

† Evaluation of SO-180 Film for Use With the KH-4B System. [redacted] (4 Aug 1969).

‡ Evaluation of SO-121 Film for Use With the KH-4B System. [redacted] (20 Nov 1969).

~~TOP SECRET~~
~~NO FOREIGN DISSEMINATION~~

This page intentionally blank.

~~TOP SECRET~~
~~NO FOREIGN DISSEMINATION~~

HANDLE VIA
~~TALENT KEYHOLE~~
CONTROL SYSTEM ONLY

2. TEST DESCRIPTION

The CR-9 aft-looking camera (unit no. 316 with second generation Petzval lens I-169) returned 7,088 feet of 3404 film plus 819 feet of SO-242 Aerial Color Film as a tag-on. All of this 3404 film was exposed through a Wratten no. 21 filter in the primary position. A material change detection (MCD) system switched the filter to its alternate position when the SO-242 material entered the active exposure mode. In the alternate position was a Wratten no. 2B filter. Because SO-242 is autonomously filtered within its own structure, the Wratten no. 2B filter was required only to maintain the focal setting of the lens, and affected the film's spectral response imperceptibly. Additionally, however, the Wratten no. 2B filter did provide a contingency safety factor for filtering out at least the most degrading blue light in the chance event of the alternate filter being called into place accidentally with the 3404 film. Photographic speed of the SO-242 is comparable to that of the black and white film, such that the given array of slit widths was adequate to cover most of the dynamic exposure range encountered on the mission for both films.

Color coverage was obtained on 13 photographic passes (213 frames) as indicated on Figs. 2-1 and 2-2. The SO-242 color portion began on frame 28 of rev D-242 (as the vehicle passed over southwest USA) and continued to the end of the mission, frame 2 of rev D-274 (over northern Texas). Processing of original SO-242 positives and production of duplicate SO-360 (Aerial Color Duplicating Film) positives were carried out at [REDACTED]

All of the passes using the color film were accomplished in the stereo mode. With 3404 film and a Wratten no. 25 filter in the forward-looking camera (unit no. 317 with third generation Petzval lens I-209), high resolution comparative coverage was obtained for most of the SO-242 frames, with the usual six-frame differential between the two cameras.

Although 51/51 T-bar, 100-foot edge, five-step gray scale and tri-color targets had been deployed for color imagery, acquisition of these deployments was unsuccessful. Ground resolution therefore had to be estimated indirectly, with the result that the sharpest color imagery produced about a 15-foot resolution level. The stereo pair 3404 original negatives produced about a 7-foot ground resolution, which is roughly a 2x difference in performance level from the SO-242 original positives. Working with dupes from both the black and white and color records, there is no difficulty in doing stereo analysis.

The first evaluation of the color imagery (at the processing site) appeared in the mission 1108-2 [REDACTED] message*:

"BALANCE AND COLOR SATURATION IS CONSIDERED GOOD. THE BEST GROUND RESOLUTION OF THE SO-242 FROM THIS MISSION APPEARS COMPARABLE TO THE BEST COLOR PROVIDED BY MISSION 1106. ALTHOUGH THE OVERALL COLOR BALANCE IS

[REDACTED] message no [REDACTED] 24 Dec 1969.

GOOD AND SLIGHT SHIFT TOWARD CYAN IS APPARENT ON SOME PASSES, THE DENSITY RANGES FROM GENERALLY MEDIUM TO SLIGHTLY HEAVY.

DEGRADATIONS TO THE COLOR MATERIAL ARE MINOR; HOWEVER, SEVERAL BLUISH COLORED MARKS ARE PRESENT INTERMITTENTLY THROUGHOUT THE MISSION. REPETITIVE SMALL YELLOW SPOTS ARE PRESENT 3.1 INCHES APART AND 1.2 INCHES FROM THE CAMERA NUMBER EDGE THROUGHOUT THE COLOR MATERIAL. THE LAST FOUR FRAMES OF THE MATERIAL CONTAIN CREASES AND ABRASIONS ASSOCIATED WITH FILM WRAP UP (i.e., depletion)."

The mission 1108 PET studied the product and produced the following PEIR message*:

"EARLY EVALUATIONS OF THE COLOR MATERIAL FROM THIS MISSION WERE CONDUCTED FROM THE COLOR DUPES AND THE RESULTING COMMENTS WERE GENERALLY NEGATIVE. THE PHOTOINTERPRETERS REPORTED THE PI SUITABILITY OF THE COLOR RECORD AS POOR FOR FIRST PHASE EVALUATIONS BECAUSE OF THE SMALL SCALE AND LOWER RESOLUTION LEVELS. THE PET FELT THAT THE BEST IMAGE QUALITY AND COLOR BALANCE OF THE ORIGINAL SO-242 ARE GOOD, BUT NOTED THAT THERE IS A SIGNIFICANT RESOLUTION LOSS FROM THE ORIGINAL TO THE DUPLICATES. MUCH OF THE SO-242 PHOTOGRAPHY APPEARED TO BE DEGRADED BY HAZE, PARTICULARLY AT THE LOW SOLAR ALTITUDES (LESS THAN 15 DEGREES). THE BEST COLOR IMAGE QUALITY WAS TAKEN AT THE HIGHER SOLAR ALTITUDES (40 DEGREES). THIS COLOR PHOTOGRAPHY IS BETTER THAN ANY OTHER COLOR PHOTOGRAPHY OBTAINED TO DATE FROM THE . . . SYSTEM, EVEN THOUGH THIS FLIGHT WAS FLOWN AT 15 PER CENT HIGHER ALTITUDE. PARTICULARLY NOTABLE WAS THE FINER DYE STRUCTURE OF THE SO-242 MATERIAL WHEN COMPARED WITH SO-121. ELECTROSTATIC FOGGING DOES NOT APPEAR TO BE A PROBLEM WITH SO-242 IN THE . . . SYSTEM."

*NPIC message no. [REDACTED] 19 Jan 1970.

~~TOP SECRET~~

NO FOREIGN DISSEMINATION

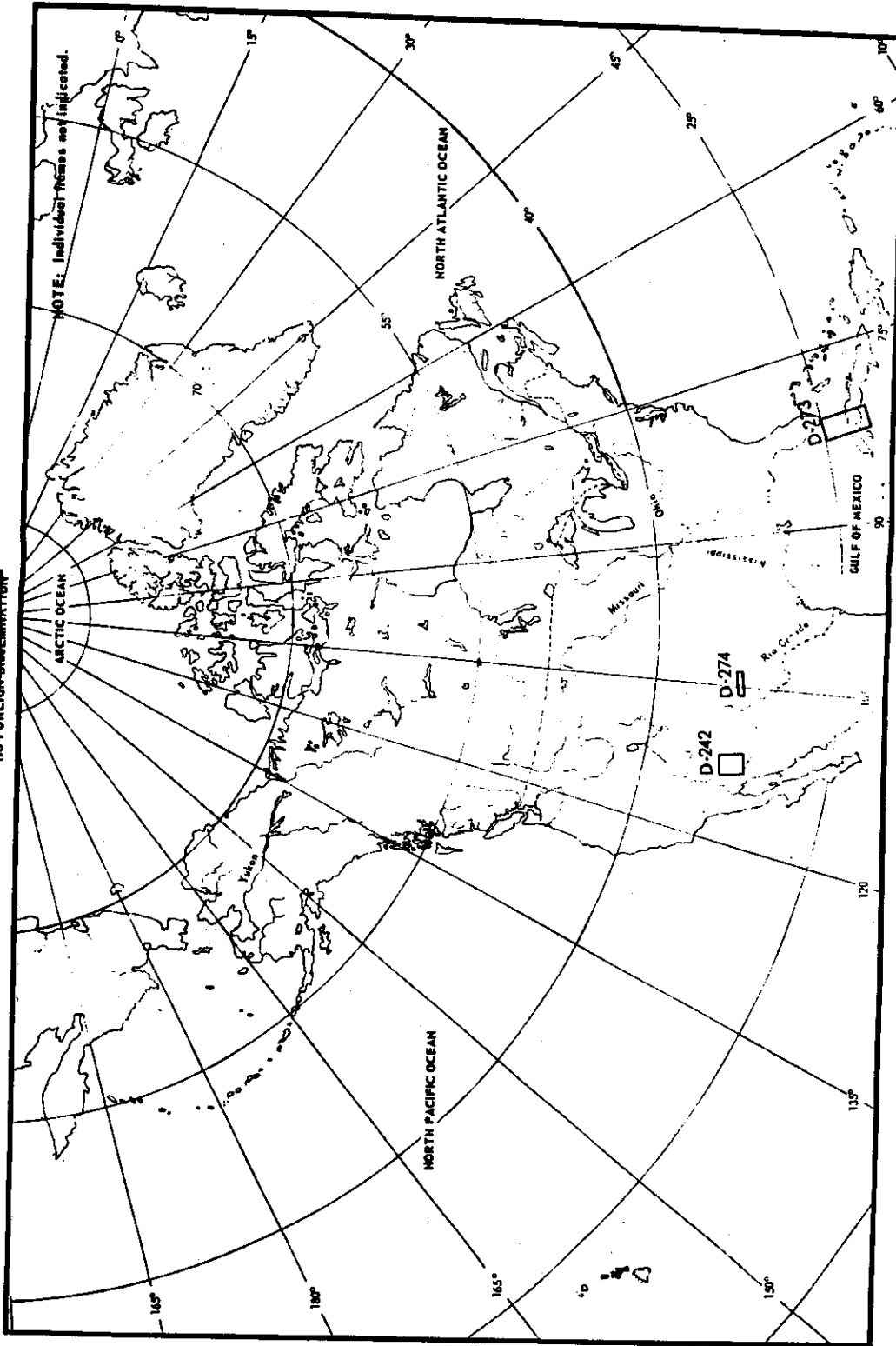


Fig. 2-1 — Ground tracks for mission 1108 SO-242 passes over the United States and Cuba

~~TOP SECRET~~

HANDLE VIA

PAGE 11

~~TOP SECRET~~
NO FOREIGN DISSEM

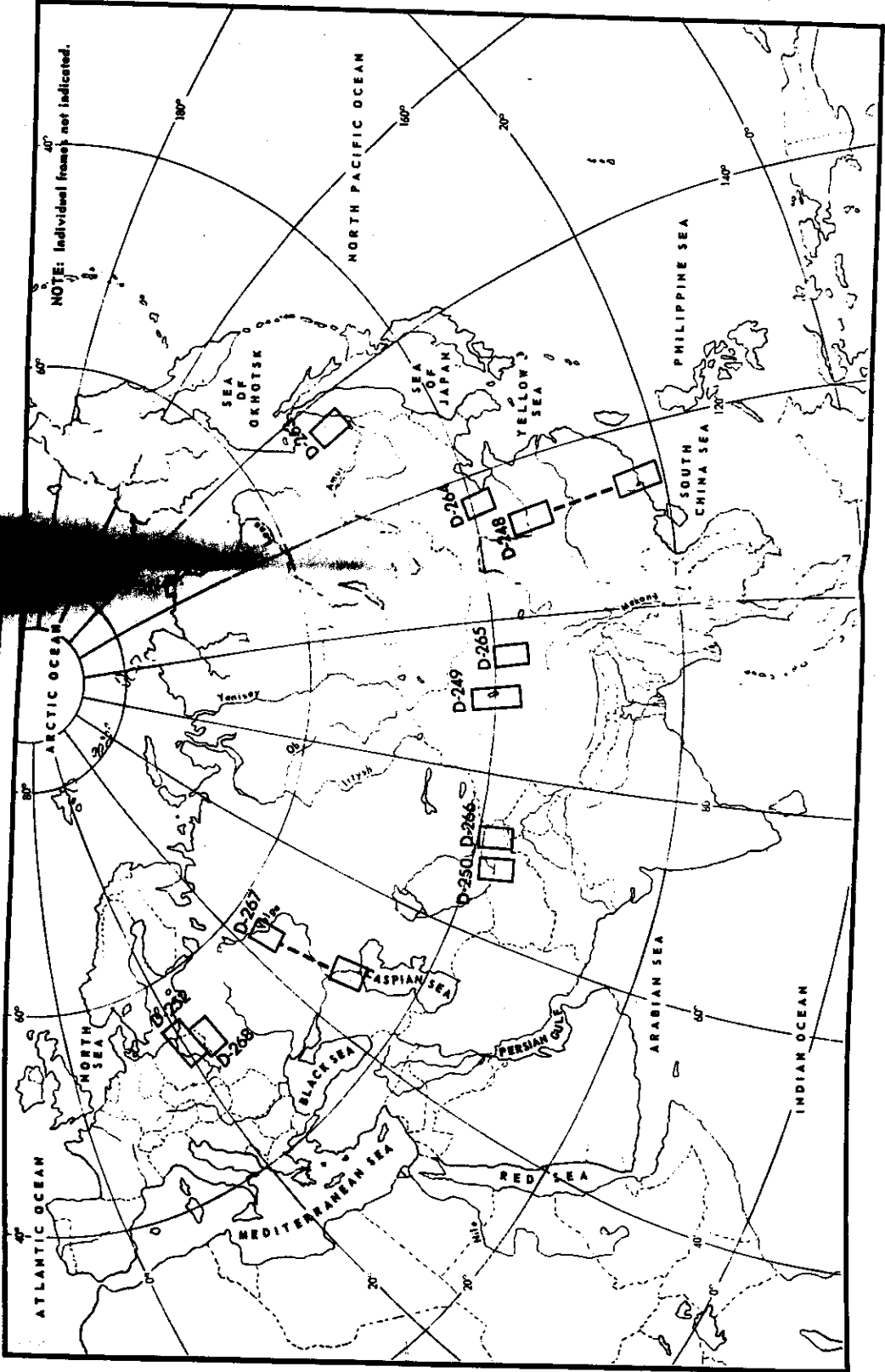


Fig. 2-2 — Ground tracks for mission 1108 SO-242 passus over Eurasia

~~TOP SECRET~~

HANDLE VIA

3. CHARACTERISTICS OF SO-242 FILM

3.1 PHYSICAL STRUCTURE

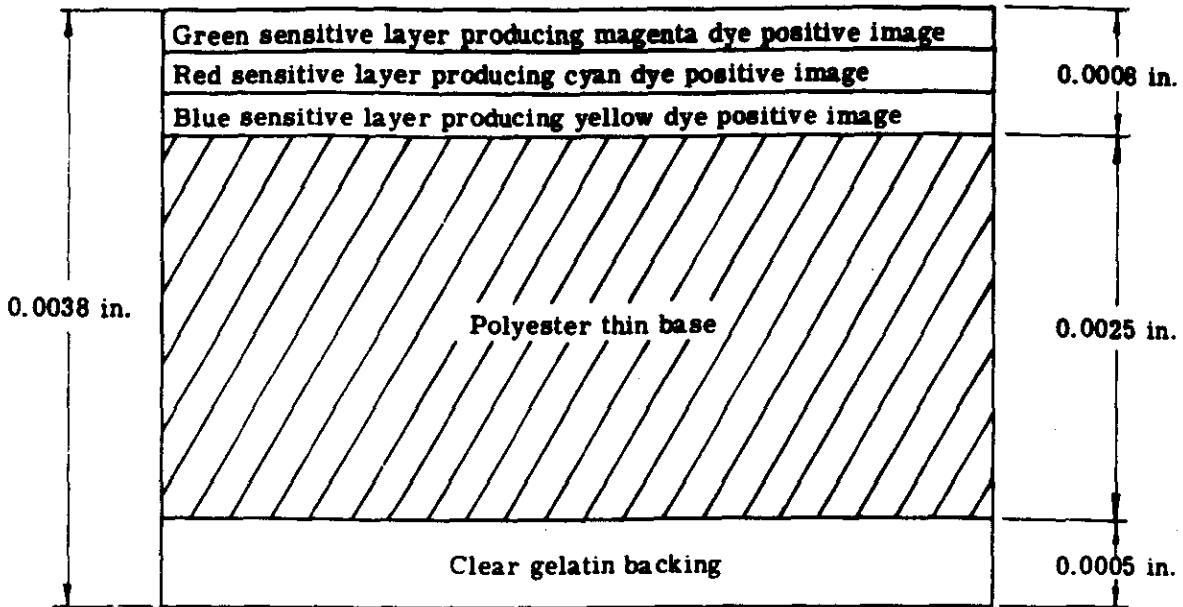
SO-242 film is an Ektachrome type emulsion on Estar thin base. The film's physical structure, illustrated in Figs. 3-1 and 3-2, accrues three sensitive layers supported by a polyester (thin) base made from polyethylene terephthalate. The ultrathin base counterpart to this film is identified as SO-255.

The three sensitive layers of silver halide suspended in gelatin of slightly different thicknesses, along with their ancillary layers, occupy a total displacement of 0.0008 inch. For anticurl provision, a clear 0.0005-inch-thick gelatin backing is included in the structure. With a base thickness of 0.0025 inch, the total thickness of SO-242 thus amounts to an average of 0.0038 inch. Variations of 0.0001 inch are within limits established by quality control during manufacture, although additional variations of less severity are introduced by fluctuations in moisture content resulting from changes in temperature and relative humidity.

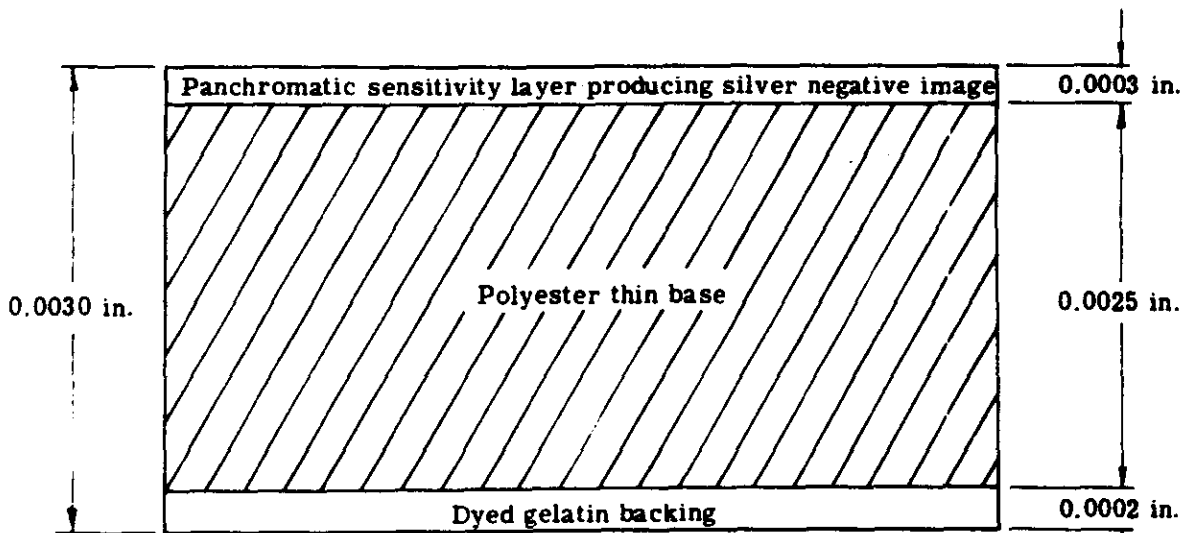
The important point is that the SO-242 color film is 0.0008 inch thicker than the 3404 black and white film. Because of this thickness difference, the film supply footage for the camera employing SO-242, full or in part, must be less than the other camera employing a full load of 3404. In the case of mission 1108, the forward-looking unit, 317, was supplied with 16,300 feet of 3404 while the aft-looking unit, 316, was supplied with 15,200 feet of 3404 and 800 feet of SO-242, resulting in 300 feet less total film footage. Utilization of the SO-255 (UTB) film in place of SO-242 would cancel this camera footage supply difference. For equal amounts of spool displacement, SO-242 footage is about 80 percent of the 3404 footage while the SO-255 footage is about 10 percent more than the 3404 footage. These observations regarding footage advantages of SO-255 (UTB tri-pack) over SO-242 (STB tri-pack) are to be qualified by the fact that the KH-4B system capability with SO-255 film has not yet been demonstrated. Considering the incompatibility of SO-380 (UTB monolayer) in the film transport mechanism of the cameras, responsible testing of the color UTB in the system would be necessary.

Image forming energy incident onto SO-242 is filtered by a Wratten no. 2B equivalent coating and then penetrates into the green sensitive, red sensitive, and blue sensitive layers, respectively (Figs. 3-1 and 3-2). The integral filtration removes the shortest wavelengths of light to which all three layers are sensitive. This arrangement of layers is different from that of either the SO-121 or SO-180 films used in previous KH-4B experiments. A comparison of the layer orientations of these three film types is given in Table 3-1. For image quality reasons revealed in Section 4, the "ideal" color film for use in the KH-4B system would have its red sensitive layer on top, followed by the green, and then yellow sensitive layers. This mythical film is included in Table 3-1 to draw the comparison out to its logical extension.

Whereas both SO-180 and SO-121 require supplementary spectral filtration, SO-242 is characterized by integral filtration. One advantage of integral filtration is a reduction in sensitivity



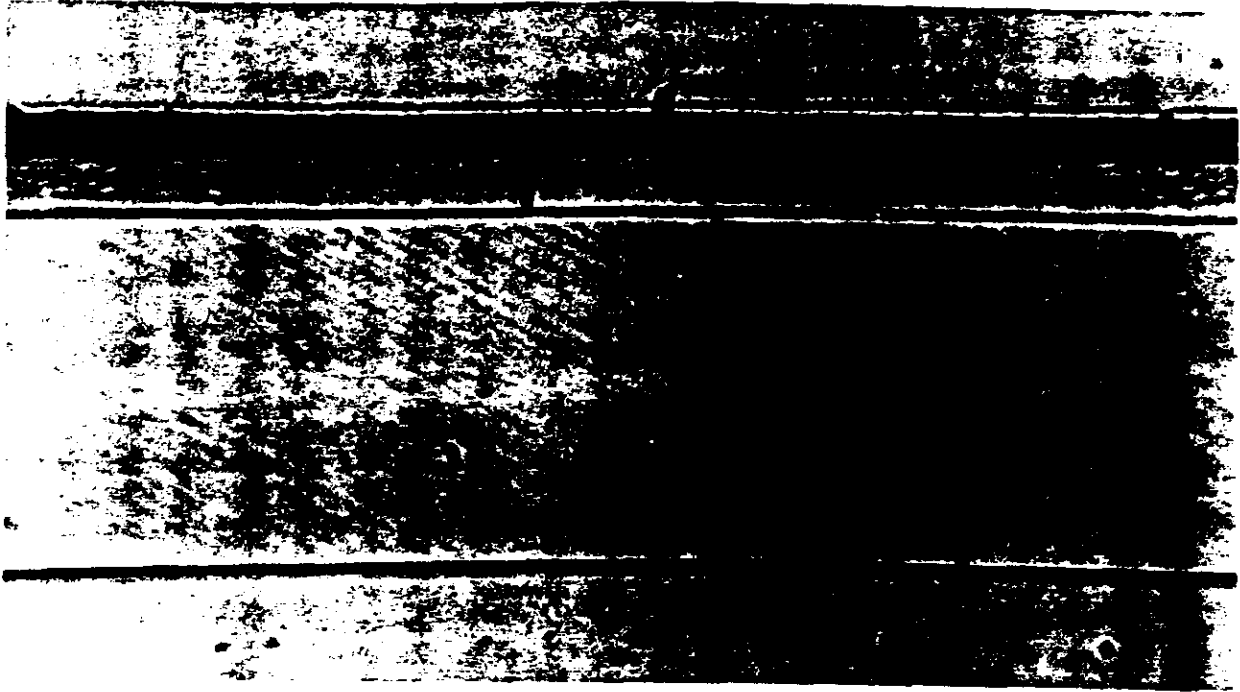
(a) SO-242 film



(b) 3404 film

Fig. 3-1 — Physical structure of SO-242 and 3404 films

~~TOP SECRET~~
~~NO FOREIGN DISSEMINATION~~



(a) SO-242 film



(b) 3404 film

Fig. 3-2 — 700× photomicrographs of cross sections of SO-242 and 3404 films

~~TOP SECRET~~
~~NO FOREIGN DISSEMINATION~~

HANDLE VIA
~~TALENT KEYHOLE~~
CONTROL SYSTEM ONLY

~~TOP SECRET~~
~~NO FOREIGN DISSEMINATION~~

This page intentionally blank.

~~TOP SECRET~~
~~NO FOREIGN DISSEMINATION~~

HANDLE VIA
~~TALENT KEYHOLE~~
CONTROL SYSTEM ONLY

Table 3-1 — Layer Orientations of the Three Color Films
Used in KH-4B Experiments

NOTE: [] indicates apart from film's structure
() indicates requirement for tag-ons only

Film	Orientation
SO-180	{ Incident light [Wratten no. 15 (+ND)] 1. Near infrared 2. Green 3. Red Base Backing
SO-121	{ Incident light [Wratten no. 2E + CC (+ND)] 1. Green 2. Blue 3. Red Base Backing
SO-242	{ Incident light [(Wratten no. 2B)] 0. Wratten no. 2B 1. Green 2. Red 3. Blue Base Backing
KH-4B "ideal"	{ Incident light 0. Filter 1. Red 2. Green 3. Blue Base Backing

to electrostatic discharge fogging during transport in KH-4B cameras, but the extent of this advantage has not been tested.

For gelatin filter KH-4B systems, use of the SO-180 and SO-121 films had to be anticipated with rather "last minute" synthesis of Wratten no. 15 plus neutral density or Wratten no. 2E plus color compensation plus neutral density filters, the transmission specifications for which were defined by the expected orbital parameters of the 1104, 1105, and 1106 missions. Now that glass filter KH-4B systems are phasing in, tailored filtration is untenable. Glass filter substrates treated with vacuum deposited dichroic interference layers have been prepared for use with integral filter color films: SO-242 (color rendition) and 3443* (color translation). These glass filters are 0.040 inch thick and will be used to maintain focal position when the alternate filter position is elected. Wratten nos. 25, 23A, and 21 type dichroic coatings on 0.040-inch substrate are available for installation in the primary filter positions. The singular purpose of the color film filters is for safety. In the event that the alternate filter position is called into place accidentally, the most detrimental short wavelengths of scattered light will be filtered out to somewhat preserve contrast and proper exposure on the black and white film, which would not be so with just clear glass.

3.2 PHOTOGRAPHIC SENSITIVITY

In order to determine the spectral sensitivity of the three recording layers composing SO-242, sample strips were exposed on an equal energy spectrosensitometer. A processed film spectrogram is reproduced in Fig. 3-3 to illustrate the film's spectral response. This reproduction is given for graphic illustration only, and does not perfectly represent the spectral information of the SO-242 transparency film. A point within the exposed area is referenced by a particular wavelength (from 400 to 700 nanometers) along the x axis and by a log exposure value (in 10 levels) along the y axis. The fact that the exposing unit is an equal energy source for the wavelength region considered allows a straightforward conversion from measured density through effective exposure to the specification of absolute spectral sensitivity. Spectral sensitivity is defined here as the reciprocal of the energy necessary to produce an analytical filter density of unity.

The SO-242 spectrogram was traced on a Mann microdensitometer to obtain integral filter density readings as a function of wavelength and exposure level. An 80-micron spot aperture was used to cover the equivalent of about 1/4-nanometer wavelength increment on the spectrogram. A total of 24 tracks were traced through exposure across the spectrogram. For each track, density was measured with respect to blue (440 nanometers), green (540 nanometers), and red (670 nanometers) filtration. Zero was referenced to base plus stain. The resulting measurements are integral filter densities.

To obtain the spectral sensitivities of the three layers independent of one another, the integral filter densities† were converted to analytical filter densities, such that the interaction of the dyes was eliminated for the remainder of the data processing. Yellow, magenta, and cyan analytical filter densities were then plotted as a function of log exposure. Because the 1.0 density level was chosen as the level for which reciprocal energy would be determined, interpolation was performed

* Kodak 3443 film is an improved version of SO-180. The 3443 film has better cyan layer speed stability with aging and moisture depletion.

† The terms "analytical filter density" (AFD) and "analytical spectral density" (ASD) are used to distinguish between measurements made with narrow band spectral filters and those made with a spectrophotometer, respectively.

on these curves to produce a log exposure value for yellow, magenta, and cyan at each of the 24 wavelengths sampled microdensitometrically. This data was then antilogged for exposure determination. The reciprocal of the exposing energy was computed for all of the determinations producing sensitivity contours for each of the three sensitive layers. A normalized version of this data is offered in Fig. 3-4 as a comparison to the spectrogram in Fig. 3-3. The absolute response data is plotted in Fig. 3-5. Sensitivity peak locations for the three layers are:

Blue = 440 nanometers
Green = 555 nanometers
Red = 655 nanometers

Comparison of SO-242 spectral sensitivity with that of its predecessor, SO-121, is offered in Fig. 3-6. The red (cyan layer) sensitivities are essentially equivalent, and the shift of the SO-242 blue (yellow layer) sensitivity towards the longer wavelengths from where it is with the SO-121 constitutes only an insignificant gain in lens modulation transfer characteristics during image formation. However, the SO-242 green (magenta layer) sensitivity is free of the SO-121 appreciable sensitivity to blue. As pointed out in the SO-121 Capability Report, this dual sensitivity not only incurs a limited blue/green discrimination capability but also results in degraded image quality in that layer due to the poor transfer of spatial frequencies in the blue spectral region. Both of these difficulties are overcome by the more selective green response of the SO-242 film.

For the purpose of determining the spectral transmission characteristics of the dyes in each of the three sensitive layers, it was convenient to fog out two of the layers, leaving the third layer to develop dye in processing to completion. To complement the three different dye layer samples produced in this way, a base-plus-stain sample, with none of the three dyes contained, was also required. Spectrophotometric traces were made of each of the three dye layer samples, with the base-plus-stain sample serving as the zero reference. This is necessary because the transmission of the base plus stain is not neutral over the spectral domain measured (Fig. 3-7). The spectral transmission traces in the 360- to 800-nanometer wavelength domain of the yellow, magenta, and cyan dyes composing SO-242 imagery were converted to density information and normalized. Results are given in Fig. 3-8. Thus, the aerial image chromatic information content incident onto the film is recorded in accordance with the spectral sensitivity of the silver halide layers (Fig. 3-5) and the processed imagery is viewed or printed in accordance with the spectral density of the dye layers (Fig. 3-8).

3.3 RESOLUTION CAPABILITY

A limited amount of testing was carried out on SO-242 film to determine its resolving power under different chromatic conditions. The results of this work are summarized by the Aerial Image Modulation (AIM) curves given in Fig. 3-9. The data for this figure were generated on a resolving power camera, the microscope objective of which introduced essentially no resolution degradation. Contrast reduction introduced by the camera, however, was taken into account such that the modulation of the aerial image presented to the film was defined. Statistical resolution levels of standard tri-bar targets were then determined for an array of incident modulation levels for white light imagery as well as for red, green, and blue imagery produced by the test camera.

The blue AIM curve is decidedly set apart, located at very low resolution levels. The red and green AIM curves have a similar shape, with the red targets being resolved consistently lower than the green targets. These tests also indicate that the green target imagery is statistically equivalent to the white light or neutral colored resolution targets. It is interesting to note the correspondence of these general resolution trends with the physical structure of the SO-242 film.

~~TOP SECRET~~
~~NO FOREIGN DISSEMINATION~~

Uppermost in the tri-pack is the green sensitive layer, with its resolution unimpeded by any intervening scattering medium. Down into the tri-pack is the comparably performing red sensitive layer, with its effective resolution level lowered somewhat because of the disadvantageous location. At the bottom of the tri-pack is the ultralow resolution capability of the blue sensitive layer.

The physical sensitometric and resolution characteristics of SO-242 film described in this chapter are applied to the KH-4B camera system in the following section.

~~TOP SECRET~~
~~NO FOREIGN DISSEMINATION~~

HANDLE VIA
~~TALENT KEYHOLE~~
CONTROL SYSTEM ONLY

Relative Log Exposure



Wavelength, nanometers

Fig. 3-3 — Reproduction of SO-242 spectrogram

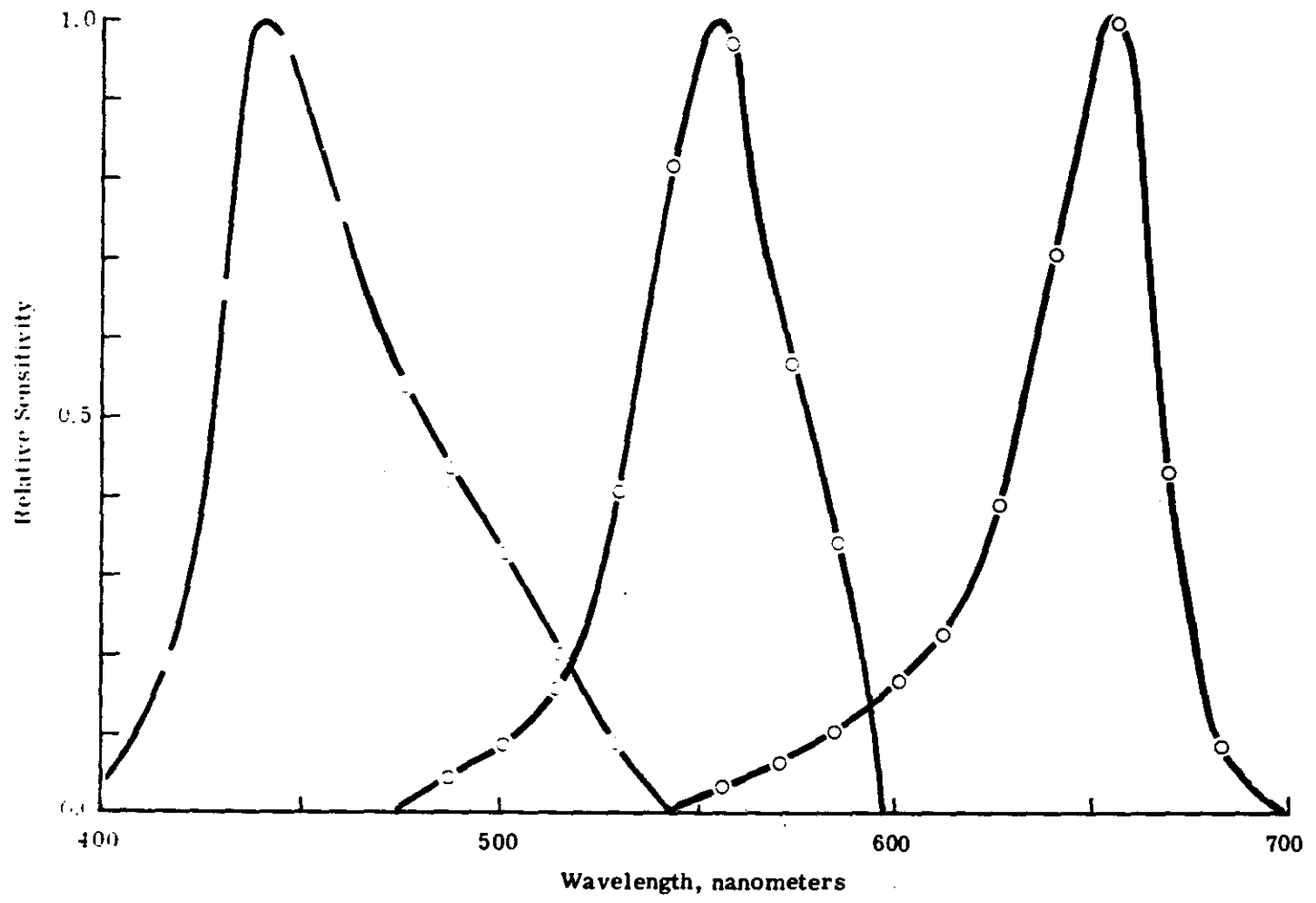


Fig. 3-4 — Spectral sensitivity of SO-242 film

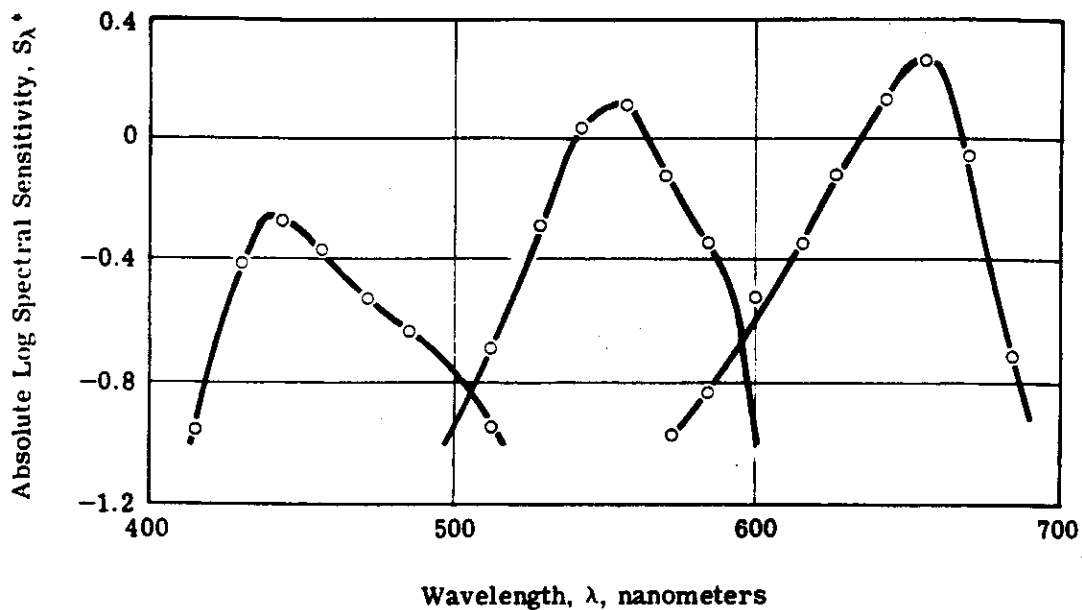


Fig. 3-5 — Absolute spectral sensitivity of SO-242 film

* $S_{\lambda} = 1/E_{\lambda}$, where E_{λ} is energy (ergs/cm²) of monochromatic light of wavelength, λ , required to reduce the dye image density in individual dye layers to an equivalent neutral density of 1.0 above minimum density.

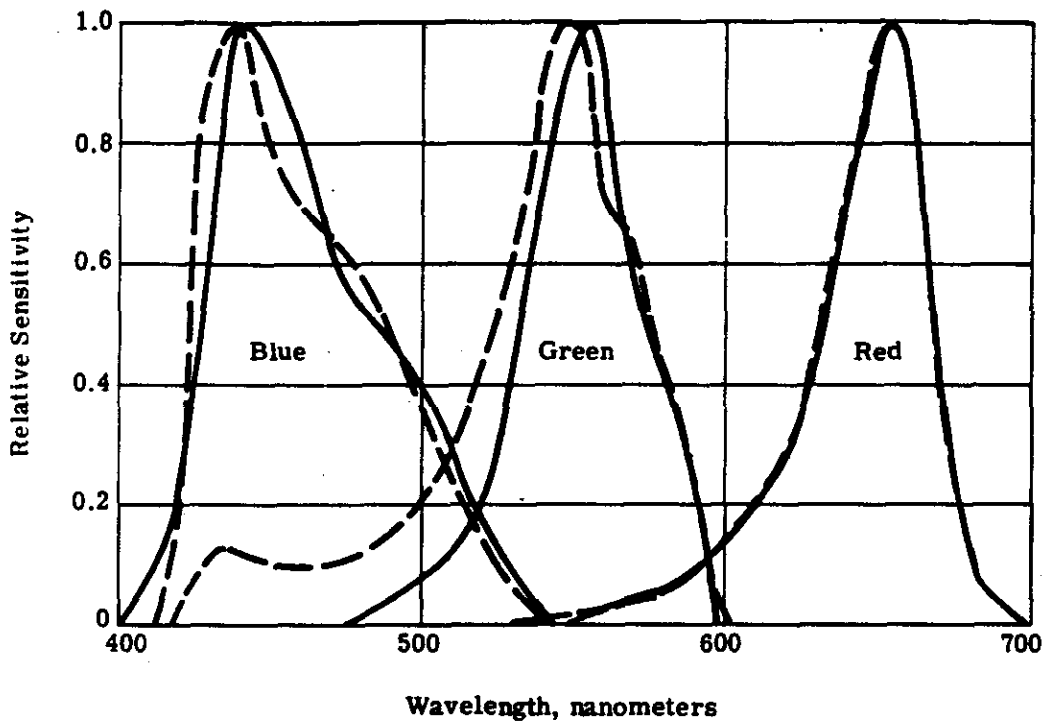


Fig. 3-6 — Normalized spectral sensitivities of SO-242 film filtered with a Wratten no. 2B and SO-121 film filtered with a Wratten no. 2E

- SO-242 (in-house determination) with external Wratten no. 2B filtration
- - - SO-121 (manufacturer's determination) with external Wratten no. 2E filtration

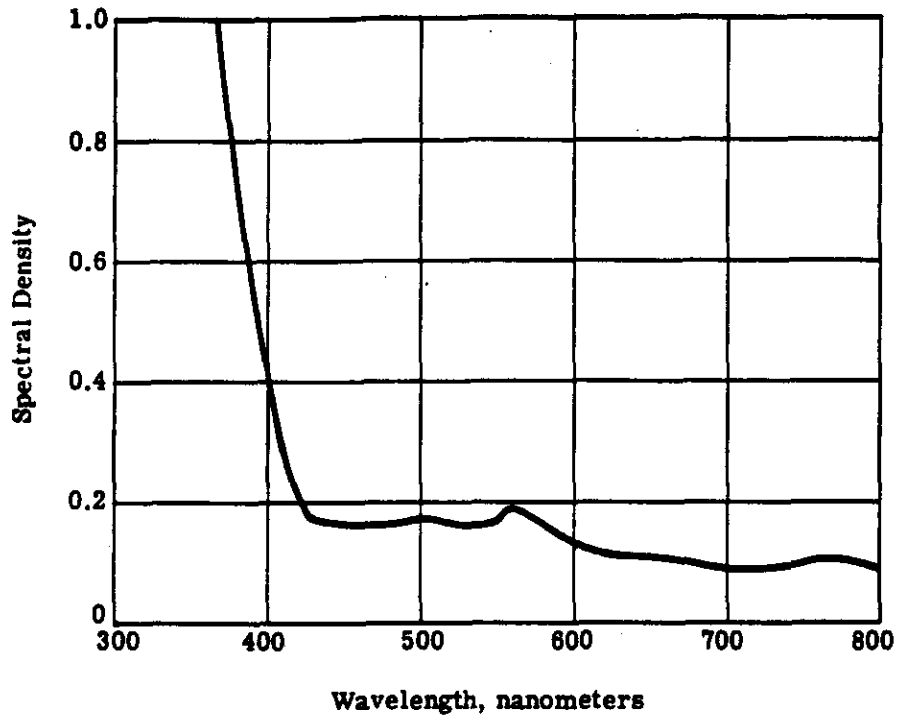


Fig. 3-7 — Spectral density of base-plus-stain of SO-242 film

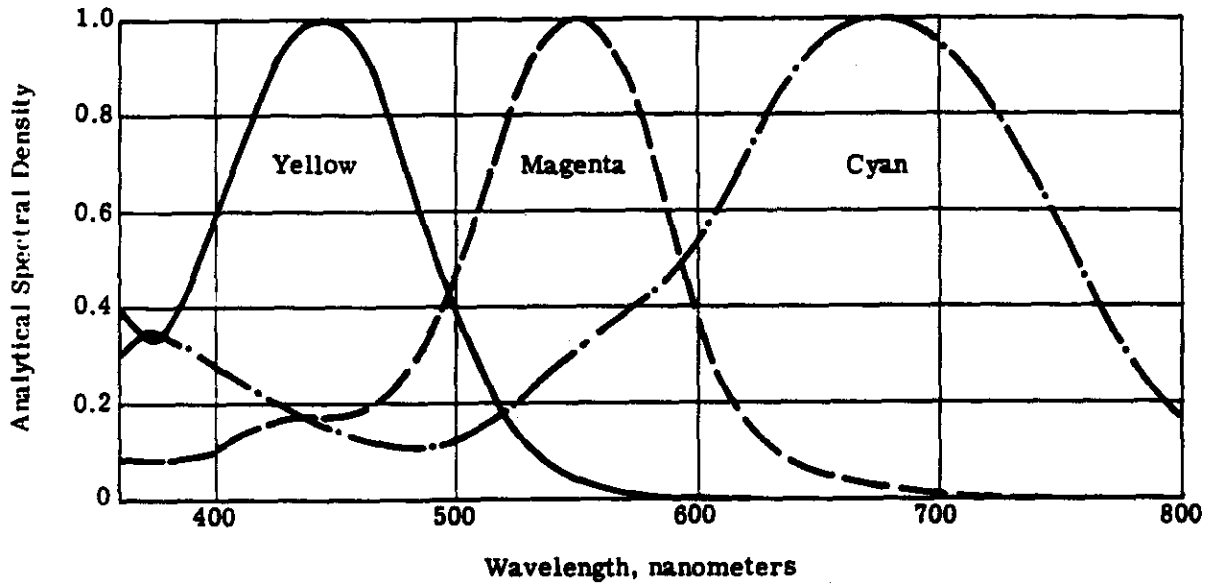


Fig. 3-8 — Dye absorption curves for SO-242 color film

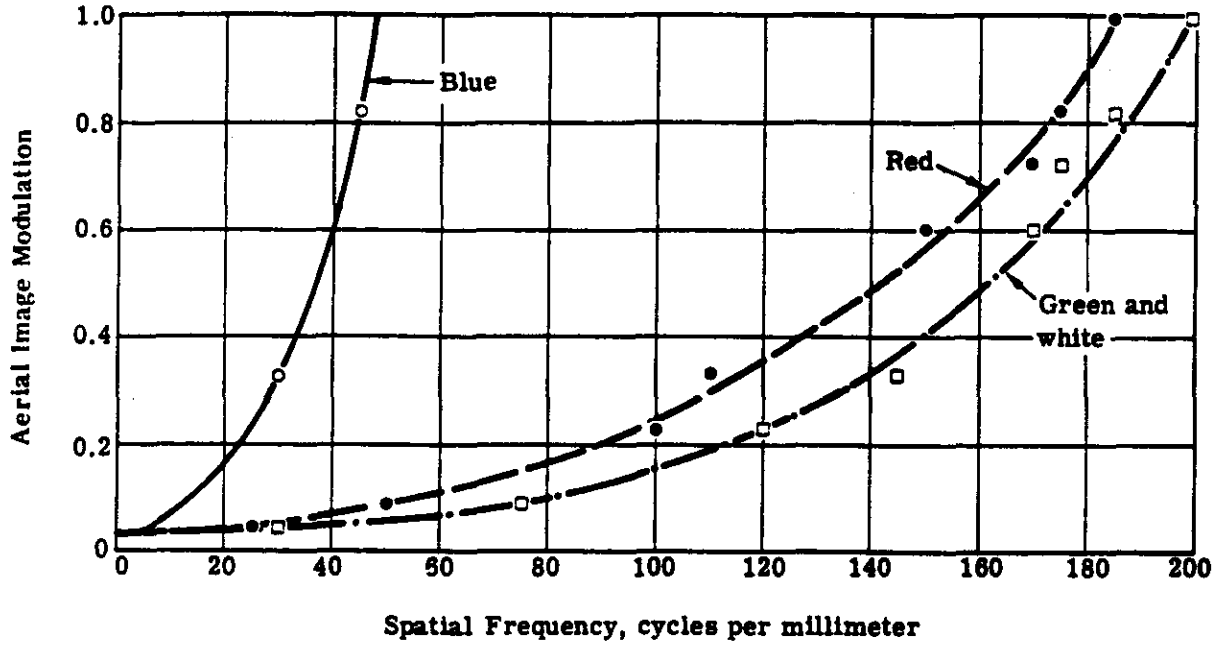


Fig. 3-9 — AIM curves for SO-242 film

4. KH-4B SYSTEM ANALYSIS WITH SO-242 FILM

4.1 PETZVAL LENS MTF's

Modulation transfer functions for second and third generation Petzval lenses are shown in Figs. 4-1 and 4-2.* Fig. 4-1 shows three transfer functions for each generation lens representing the spectrally weighted lens MTF's for the red, green, and blue isolated sensitivities of the SO-242 emulsion layers. Fig. 4-2 shows three transfer functions for each generation lens for monochromatic wavelengths chosen at the peak sensitivities of the three SO-242 layers. In Fig. 4-3 the spectral sensitivities of the three SO-242 layers (as determined in Section 3.2) are shown. The contours superimposed on these spectral sensitivity curves represent modulation transfer as a function of wavelength at two spatial frequencies (10 and 100 cycles per millimeter) for both second and third generation lenses.

Since the blue sensitive response of SO-242 is almost entirely on the outside of these modulation transfer contours, it is evident that the MTF in any portion of this spectral region will be very poor. The green spectral region is more complex. The lens modulation transfer varies through this region such that the spectral composition of the light has an important bearing on the image formation. As a consequence, objects having different green hues will be imaged with different spatial frequency content and therefore different image quality. In the red region, on the other hand, the modulation transfer contours tend to weight the inclusive wavelengths equally. The implication here is that the actual wavelength composition of red objects has much less effect on the final image structure than objects in the green spectral region.

It is also evident from Fig. 4-3 that the second generation lens will perform better than the third generation lens in the green spectral region because modulation transfer values are consistently higher at any wavelength in the 500- to 600-nanometer region. This comparison is also reflected in Figs. 4-1 and 4-2. For red light, this clear-cut distinction is nonexistent. The similarity of the contours in this spectral region tends to result in rather similar performance. However, in Figs. 4-1 and 4-2 the second generation lens is shown to be better at the low spatial frequencies, whereas the third generation lens is shown to be better at the higher spatial frequencies. Because most of the imagery produced in the KH-4B system on SO-242 film is composed of spatial frequencies below 100 cycles per millimeter, the superiority of the second generation lens is suggested.

4.2 SO-242 DYE LAYER ISOLATION

In order to understand what is happening in each of the three emulsion layers of SO-242 the individual cyan, magenta, and yellow dye images must be isolated. A partial isolation can be achieved by viewing the transparency through red, green, or blue separation filters or by printing separate black and white records using the same filters. These procedures produce only a partial

* Note that the blue MTF's in Figs. 4-1 and 4-2 are estimated from geometric considerations based on a defocus condition.

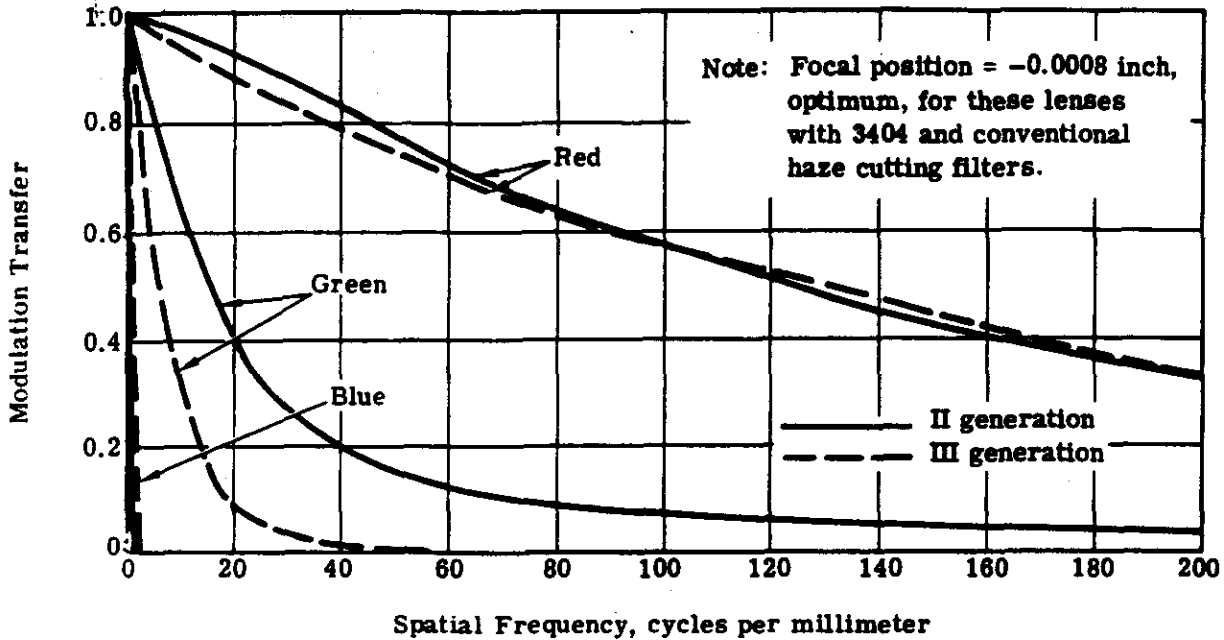


Fig. 4-1 — MTF's for second and third generation Petzval lenses for the three spectral sensitivities of SO-242 film

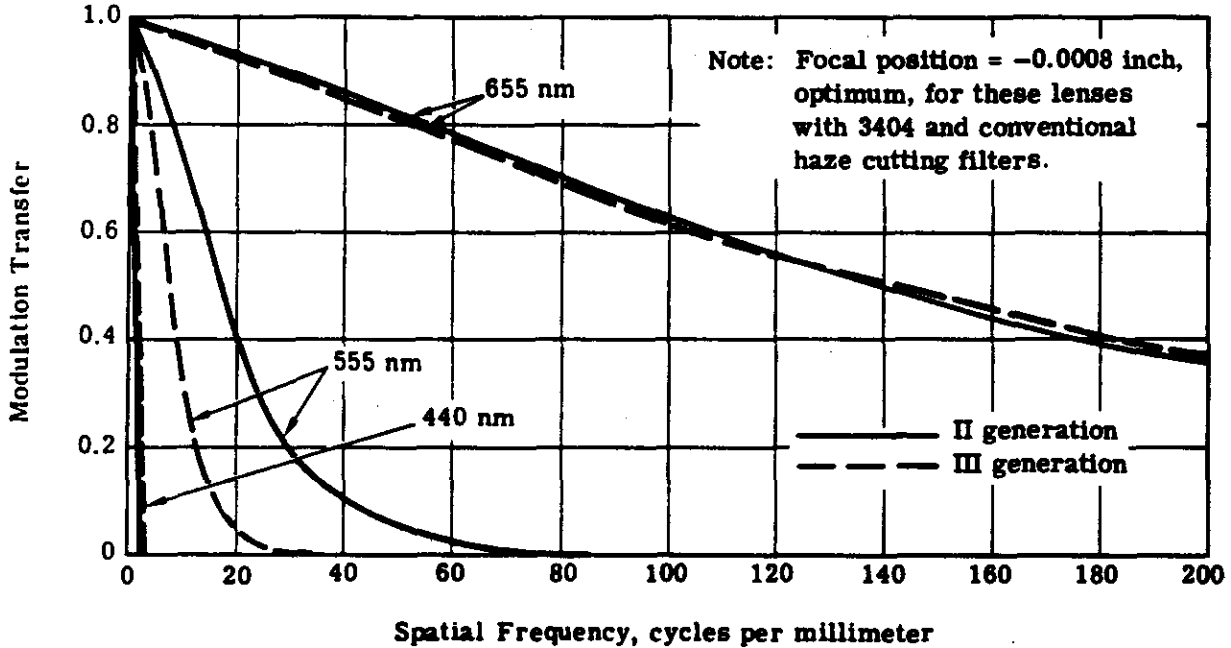


Fig. 4-2 — MTF's for second and third generation Petzval lenses for three wavelengths at the sensitivity peaks of SO-242 film

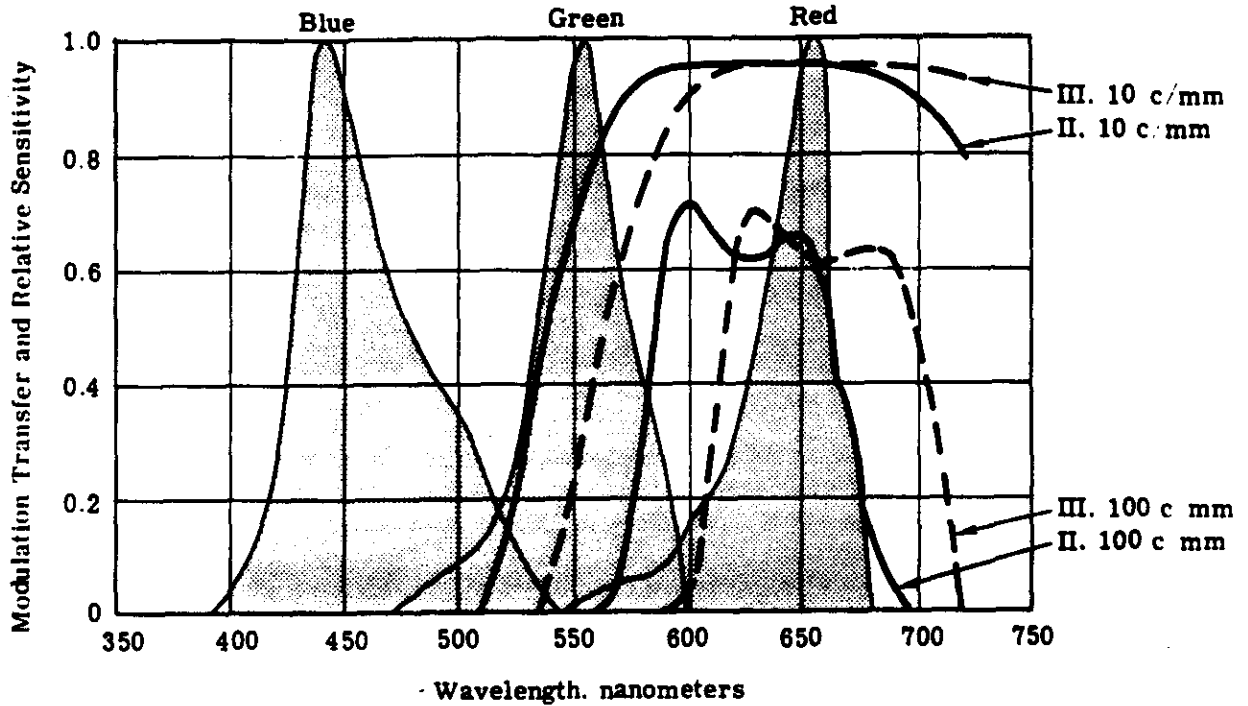


Fig. 4-3 — Comparison of Petzval lens modulation transfer contours

———— II generation
- - - - III generation

Note: Modulation transfer for both second and third generation Petzval lenses was determined at best focus for 3404 with Wratten nos. 21 and 25, respectively.

separation due to the interlayer interaction of the dyes, as can be seen in Fig. 3-8. For example, when viewing or printing a color image with green light, most of the modulation is controlled by the magenta dye. However, there is some modulation being controlled by the yellow and cyan dyes as well.

In an ideal tri-pack color film, the dyes associated with the three layers would have spectral absorption distributions that were totally independent. In practice, however, this condition is never realized. A vector representation of the spectral density distributions of the dye layers can be used to determine a quantitative measure of the degree of independence of the layers. Values of the SO-242 normalized spectral density distribution (Fig. 3-8) of the individual dyes taken at 10-nanometer intervals were used as coefficients for unit vectors associated with the various wavelengths. For example, at $\lambda = 510$ nanometers, the spectral density coefficients are $C = 0.16$, $M = 0.60$, and $Y = 0.27$. The generalized equations are as follows:

$$\begin{aligned}\bar{Y} &= y_1 \bar{\lambda}_{360} + y_2 \bar{\lambda}_{370} + y_3 \bar{\lambda}_{380} + \dots + y_{45} \bar{\lambda}_{800} \\ \bar{M} &= m_1 \bar{\lambda}_{360} + m_2 \bar{\lambda}_{370} + m_3 \bar{\lambda}_{380} + \dots + m_{45} \bar{\lambda}_{800} \\ \bar{C} &= c_1 \bar{\lambda}_{360} + c_2 \bar{\lambda}_{370} + c_3 \bar{\lambda}_{380} + \dots + c_{45} \bar{\lambda}_{800}\end{aligned}\tag{4.1}$$

where \bar{C} , \bar{M} , and \bar{Y} refer to the cyan, magenta, and yellow dyes, respectively, and $\bar{\lambda}$ is the unit vector associated with the various wavelengths. This procedure was performed for the spectral region extending from 360 to 800 nanometers. Direction cosines were then calculated for the three possible dye-pair interactions:

$$\begin{aligned}\cos(\theta)_{yc} &= \frac{\bar{Y} \cdot \bar{C}}{|\bar{Y}| |\bar{C}|} \\ \cos(\theta)_{mc} &= \frac{\bar{M} \cdot \bar{C}}{|\bar{M}| |\bar{C}|} \\ \cos(\theta)_{ym} &= \frac{\bar{Y} \cdot \bar{M}}{|\bar{Y}| |\bar{M}|}\end{aligned}\tag{4.2}$$

where the numerators are vector dot products and the denominators are products of vector magnitudes.

The results for the SO-242 dye layer interactions are:

$$\begin{aligned}\cos(\theta)_{yc} &= 0.2127 \\ \cos(\theta)_{mc} &= 0.3797 \\ \cos(\theta)_{ym} &= 0.3363\end{aligned}\tag{4.3}$$

such that

$$\begin{aligned}\theta_{yc} &= 77^\circ 41' \\ \theta_{mc} &= 67^\circ 41' \\ \theta_{ym} &= 71^\circ 25'\end{aligned}\tag{4.4}$$

This technique gives a quantitative measure of the degree of dependence of the dye layers. Dyes that are totally independent would yield a direction cosine of zero ($\theta = 90$ degrees), demonstrating orthogonality. At the other extreme, a direction cosine of unity ($\theta = 0$ degrees) would represent total interaction or a repetition of the dye itself. In actual films, direction cosines are somewhere between these two hypothetical conditions. Eqs. 4.3 and 4.4 reveal that for SO-242 film the interaction between the yellow and cyan dyes is least severe, while the interaction between the magenta and cyan dyes is most severe. As can be observed in Fig. 3-8, the spectral density distributions of the yellow and magenta dyes tend to be narrow and localized, whereas the cyan dye is broad and spread out. Because of this encompassing cyan distribution, the cyan dye is involved in both the greatest and the least interactions.

4.3 INTEGRAL AND ANALYTICAL FILTER DENSITIES

When a microdensitometer is used with narrow band spectral filters to measure the red, green, and blue densities of a color film tri-pack, it effectively measures the major density contribution of the dye having maximum absorption to the spectral region being considered, but it also measures minor density contributions from the other two dye layers. These densities are known as integral filter densities (IFD's). The major contribution to the red, green, and blue densities (D_R , D_G , D_B) is from the cyan, magenta, and yellow dyes respectively. Therefore, making the assumption that the spectral density of the dye is proportional to the concentration of the dye (Beer's Law), the following equations can be written:

$$\begin{aligned} D_B &= A_{11} Y + A_{12} M + A_{13} C \\ D_G &= A_{21} Y + A_{22} M + A_{23} C \\ D_R &= A_{31} Y + A_{32} M + A_{33} C \end{aligned} \tag{4.5}$$

where A_{ij} is the coefficient for the density contributions of a particular dye to a particular "color" density, i.e., D_B , D_G , D_R .

These equations can be expressed as a matrix multiplication

$$\begin{bmatrix} D_B \\ D_G \\ D_R \end{bmatrix} = \begin{bmatrix} A_{11} & A_{12} & A_{13} \\ A_{21} & A_{22} & A_{23} \\ A_{31} & A_{32} & A_{33} \end{bmatrix} \cdot \begin{bmatrix} Y \\ M \\ C \end{bmatrix} \tag{4.6}$$

Therefore, in order to obtain the densities associated with the individual dye layers termed analytical filter densities (AFD's) and denoted here as Y , M , and C , it is necessary to take the inverse of the absorption coefficient matrix.

$$\begin{bmatrix} Y \\ M \\ C \end{bmatrix} = \begin{bmatrix} A_{11} & A_{12} & A_{13} \\ A_{21} & A_{22} & A_{23} \\ A_{31} & A_{32} & A_{33} \end{bmatrix}^{-1} \cdot \begin{bmatrix} D_B \\ D_G \\ D_R \end{bmatrix} \tag{4.7}$$

The absorption coefficient matrix $[A_{ij}]$ is determined by completely fogging two of the three dye layers and exposing a step tablet in the third dye layer. Red, green, and blue densities are then measured using the narrow band spectral filters previously mentioned to obtain the integral filter densities (IFD's). This results in three sensitometric curves for each dye layer, one for

the major density and one for each of the minor densities. Minor density values are then plotted against the major density values. Since a linear relationship exists over an extended range, the slopes (γ in Fig. 4-4) of the lines are taken as the normalized density coefficients. This procedure is repeated for each of the three dye layers. Since the major densities are plotted against themselves, their slope is unity, which results in an absorption coefficient matrix which has diagonal values of unity. Fig. 4-4 shows the minor densities plotted against major densities for each of the three dye layers as they were measured for SO-242 film. The absorption coefficient matrix for SO-242 film so determined was:

$$[A_{ij}] = \begin{bmatrix} A_{11} & A_{12} & A_{13} \\ A_{21} & A_{22} & A_{23} \\ A_{31} & A_{32} & A_{33} \end{bmatrix} = \begin{bmatrix} 1.000 & 0.066 & 0.023 \\ 0.172 & 1.000 & 0.043 \\ 0.069 & 0.069 & 1.000 \end{bmatrix} \quad (4.8)$$

This matrix was used in the determination of AFD's for all the work in the following sections.

4.4 SIGNAL AND NOISE PERTURBATIONS

In order to ensure that comparisons made between transfer functions for the three dye layers were representative, a neutral edge and step tablet made on a monochrome material were traced on the microdensitometer using the three narrow band spectral filters employed in the color work. The microdensitometer was refocused for each color. This is particularly necessary for the blue spectral region, since the achromat microscope objectives are not corrected for blue light. The transfer functions determined from these edge traces represent lens/film/microdensitometer combined transfer functions.

Since the lens/film transfer function used in making the test edge was not known, the microdensitometer MTF could not be determined directly. As an indirect estimation, the measured white light transfer function was converted to a previously accepted standard instrument MTF, and the conversion coefficients applied to the other "color" transfer functions as well (results are plotted in Fig. 4-5).

Transfer functions for the white, green, and blue regions are essentially the same. The marked deviation of the red transfer function, however, made it necessary to remove its influence from the Petzval lens/cyan dye layer transfer functions. The effect on the Petzval lens/cyan dye layer transfer function, although significant, is not large. For example, the difference between the corrected and uncorrected average Petzval lens/cyan layer MTF lies within the range of the data (Fig. 4-9). Although this experiment clearly shows a significantly lower instrument response in the red spectral region, it is the result of a single experiment and should be verified by measuring the instrument transfer function directly.

Transfer functions for the Petzval lens/SO-242 film layers indicate how the signal will be affected in the various dye layers. The quality of the image in a layer, however, cannot be described by transfer functions alone since the information available will be a function of the signal/noise interaction.

To illustrate the noise characteristics in each of the dye layers, red, green, and blue traces (176- by 1-micron slit) were made on SO-242 "neutral" density areas. The data was sampled at 1-micron intervals and converted to AFD's for plotting (see Fig. 4-6). Two different density levels were utilized in order to illustrate the noise characteristics at both high and low density levels. The yellow dye layer is much noisier than the other two dye layers, particularly at the high density. The effect of this high noise level will become evident in the following section.

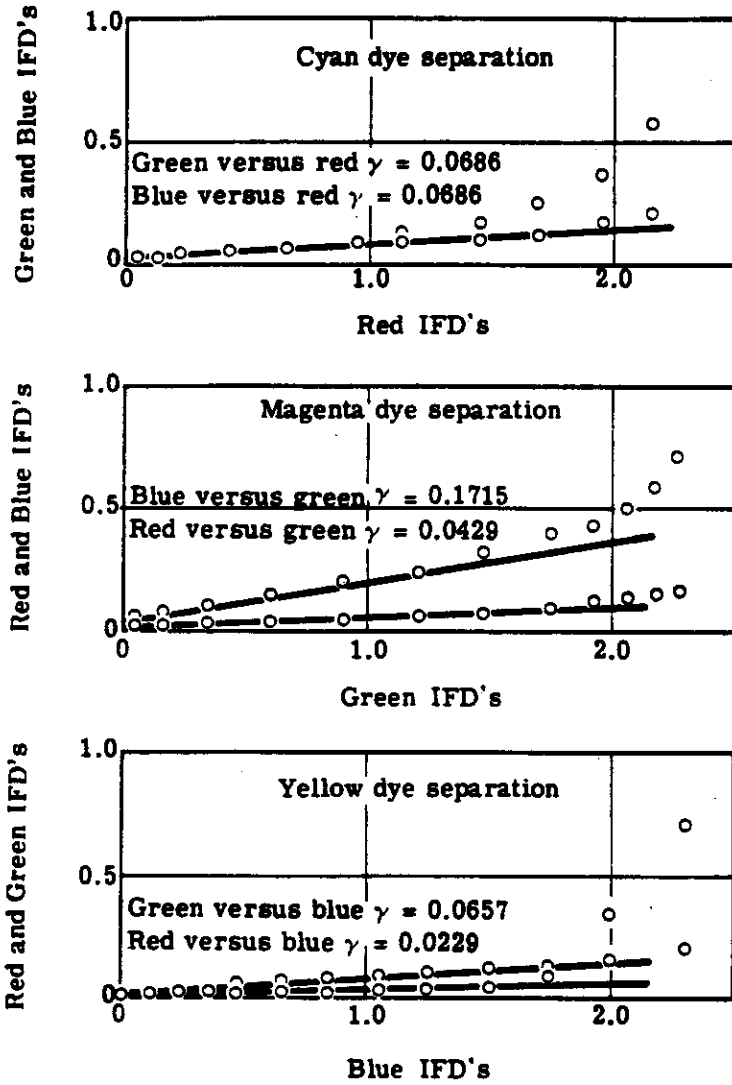


Fig. 4-4 — Minor/major density plots for SO-242 film

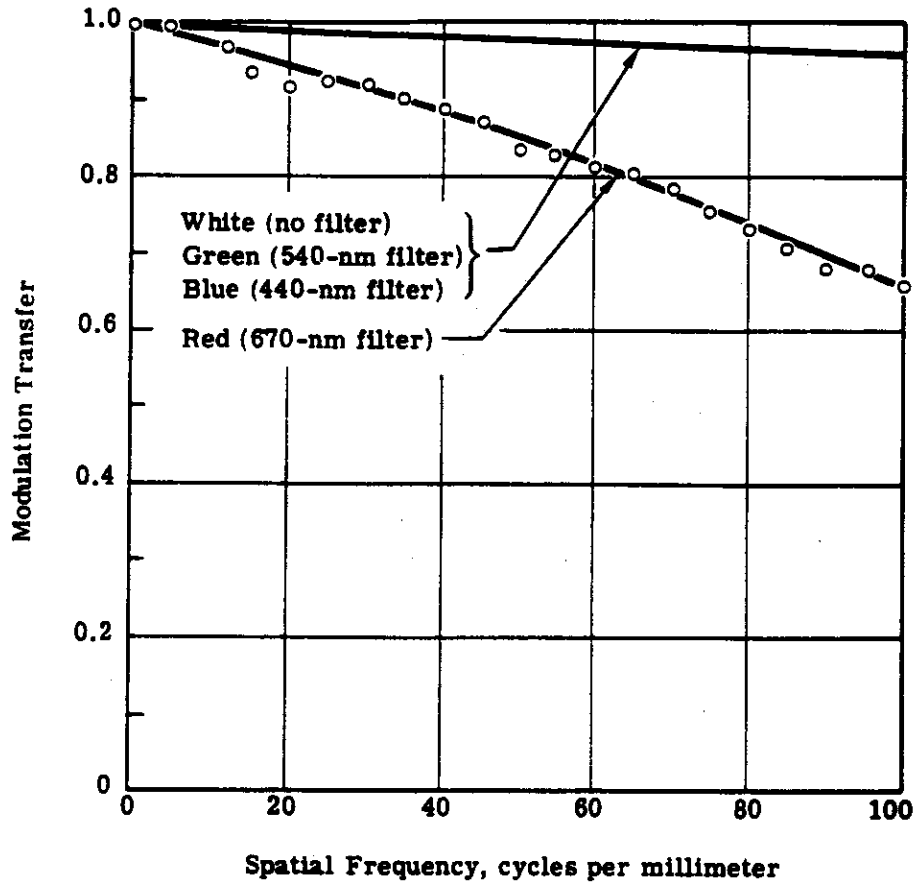


Fig. 4-5 — Microdensitometer MTF's for several spectral bands

TOP SECRET
SECURITY INFORMATION

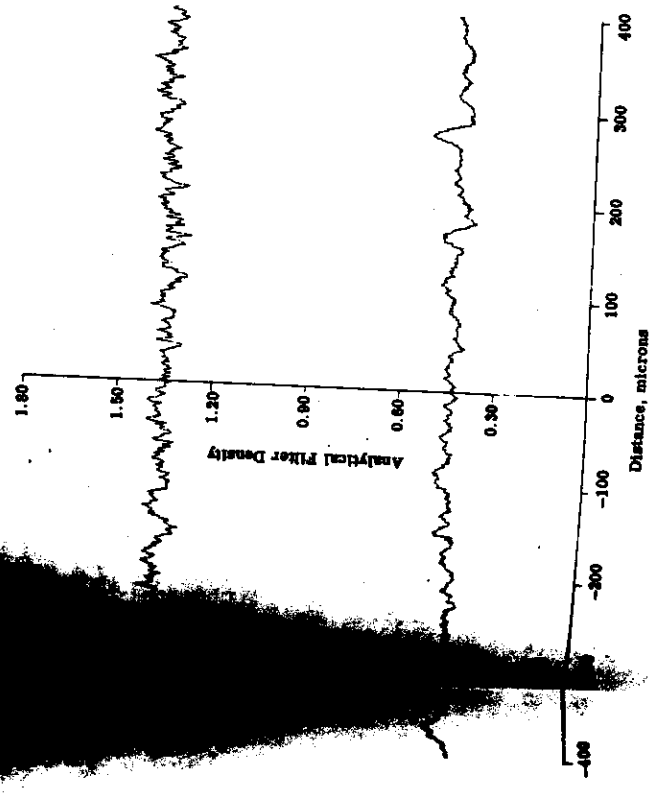
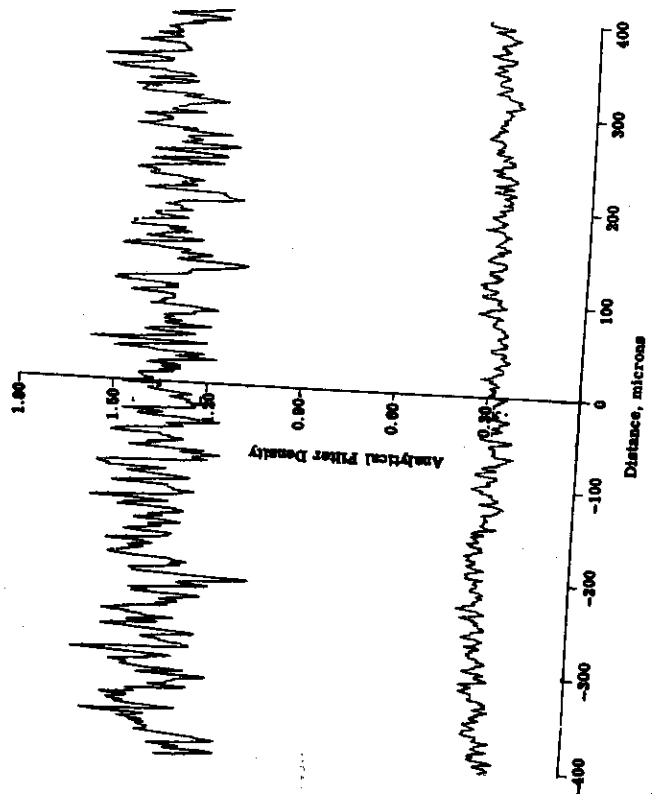


Fig. 4-6 — Photographic noise characterization in 80-242 film

TOP SECRET
NO FORN DISSEMINATION

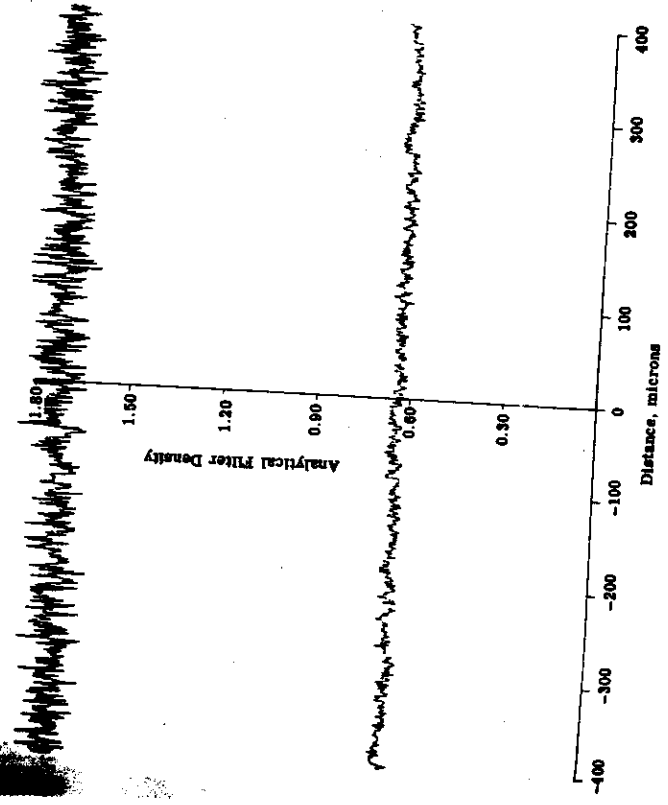
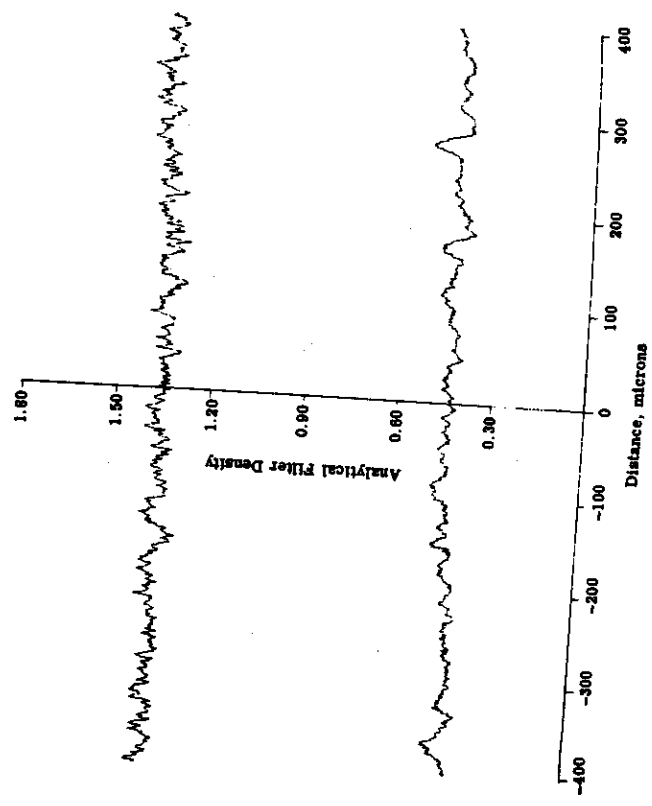


Fig. 4-6 — Photographic noise characterization in SO-242 film

The low frequency ripple present in the green and absent in the red was unexpected. However, scattering and shadowing caused by the silver halide particles in the magenta dye layer during exposure certainly affects the light distribution in the cyan dye layer. In addition, the measurements were made with the pelloid backing in place.

4.5 LENS/LAYER MTF DETERMINATIONS

In order to obtain an indication of the image quality capability of the KH-4B system with SO-242 film, transfer functions were determined from edge traces using imagery obtained with both second and third* generation lenses on the color film. Edges of photometric patches associated with imagery of low contrast (2:1) tri-bar targets were traced on the Mann microdensitometer with a 176- by 1-micron slit. The microdensitometer was equipped with three narrow band spectral filters having peak transmissions at 440, 540, and 670 nanometers in order to obtain IFD's for the SO-242 color film tri-pack. The appearance of an edge as viewed through narrow band spectral filters (IFD distributions) is illustrated in Fig. 4-7. IFD's were converted to AFD's (Section 4.3) and these values were converted to effective exposure using the sensitometry associated with the film strips. Once the effective exposure distribution of the edge had been determined, edge gradient analysis procedures† were employed. Fig. 4-8 shows a microdensitometer trace (IFD) of an edge, the analytical density distribution determined for the dye layer, its effective exposure distribution, and the transfer function determined for the lens/layer combination. In this particular illustration, the imagery was produced with a third generation lens and the distributions shown are for the cyan dye layer only. Analogous procedures were followed for all lens/layer combinations.

Composites of the replicate determinations of the lens/layer transfer functions for the cyan and magenta dye layers for both second and third generation lenses appear in Fig. 4-9. From these plots, the degree of experimental error in measuring these MTF's may be inferred. In Fig. 4-10 the IFD and AFD distributions are shown for the blue sensitive yellow dye layer. The transfer function is not presented, however, since the signal-to-noise ratio is so low even at spatial frequencies of 1 or 2 cycles per millimeter that a meaningful determination is not possible. The blue sensitive layer, being the bottom layer of the tri-pack, is also more susceptible to non-linear effects such as adjacency. This complicates an accurate determination of the transfer function, since this nonlinearity is not removed by conventional sensitometry. Indications are, however, that there is a signal record in the blue sensitive layer, but its prime importance with this system is in terms of contributing to color balance and not to the resolution capability.

In Fig. 4-11, averages of the lens/layer transfer functions for the cyan and magenta dye layers are presented for both the second and third generation lenses. The important conclusion from this data is the fact that the lens/layer transfer function associated with the red sensitive cyan dye layer is limited by the film, whereas the green sensitive magenta dye layer is limited by the lens. This becomes apparent when the lens and lens/layer transfer functions are compared (see Figs. 4-1 and 4-11).

The fact that the green MTF's in both figures are essentially the same is associated with the out of focus condition of the magenta dye layer when the system is focused for red filtered

* Although the lens actually used to produce the imagery for this part of the work was a fourth generation (I-225) system, there is no discrepancy in making correlations with the calculations in Section 4.1.

† Blackman, Elliot S., Recovery of System Transfer Functions from Noisy Photographic Records. SPIE Image Information Recovery Seminar Proceedings, Philadelphia, Penn. (24-25 Oct 1968).

~~TOP SECRET~~

~~NO FOREIGN DISSEMINATION~~

3404 film. The situation is depicted in Fig. 4-12 in which the focal positions of the peak sensitivity wavelengths are located on the optical axis of a second generation Petzval lens. Using geometric considerations only to simplify the point, it is clear that the size of the blur circles for the actinic radiation in each of the three sensitive layers are each different by an order of magnitude. Red light is focused in the magenta layer (at F_r), but this is only 0.0002 inch in front of the cyan layer such that the blur circle diameter is $d_r = 2$ microns. Green light is focused behind the film (at F_g) with the consequent blur circle diameter being $d_g = 39$ microns. Blue light is focused far down the optical axis (at F_b) creating a huge $d_b = 555$ -micron blur circle diameter.

That the red MTF's are very much lower for the lens/layer combination (Fig. 4-11) than they are for the case of the lens alone (Fig. 4-1) is explained by a film MTF reduction in the cyan dye layer itself and the fact that light is incident on the red sensitive layer through a scattering medium, i.e., the green sensitive upper layer. It is therefore suspect to characterize image formation within integral layers using linear analysis since the scattering caused by the silver halide particles in the intervening layers is object dependent, that is, the scattering is dependent upon the light color and distribution and therefore its influence varies from point to point. The superiority of the second generation lens over the third generation lens suggested in Section 4.1 is now well defined by the lens/film transfer functions determined experimentally. Mission 1108 color imagery was acquired with a second generation lens.

For future tag-ons for which the system is focused for monolayer film, the performance level of the SO-242 color imagery with third or fourth generation lenses can not be expected to exceed that of the mission 1108 experiments. However, for a full load of color film in which the system is focused for an optimum tradeoff between the red and green layers, an improved performance is indicated.

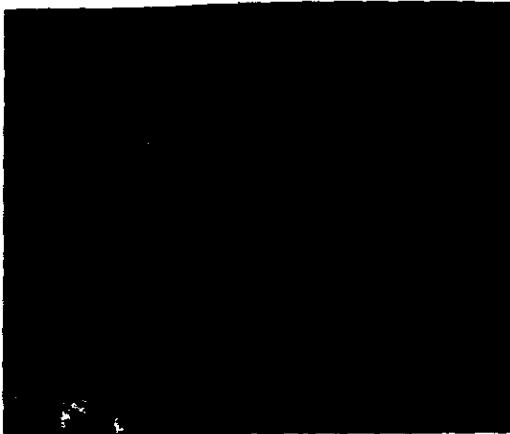
~~TOP SECRET~~

~~NO FOREIGN DISSEMINATION~~

HANDLE VIA

~~TALENT KEYHOLE~~

CONTROL SYSTEM ONLY



(a) Magenta dye layer, Wratten no. 99 filter



(b) Cyan dye layer, Wratten no. 29 filter



(c) Yellow dye layer. Wratten no. 47B

Fig. 4-7 — 450× enlargements of an edge imaged in SO-242 film reproduced through red, green, and blue filters

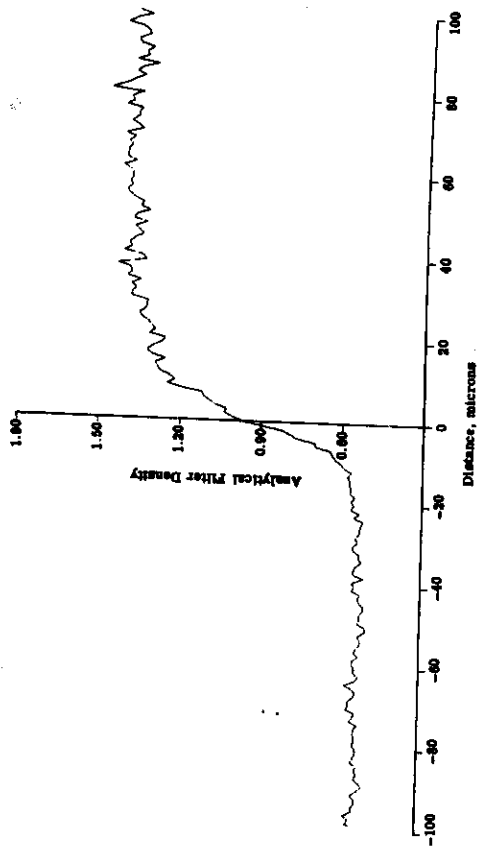
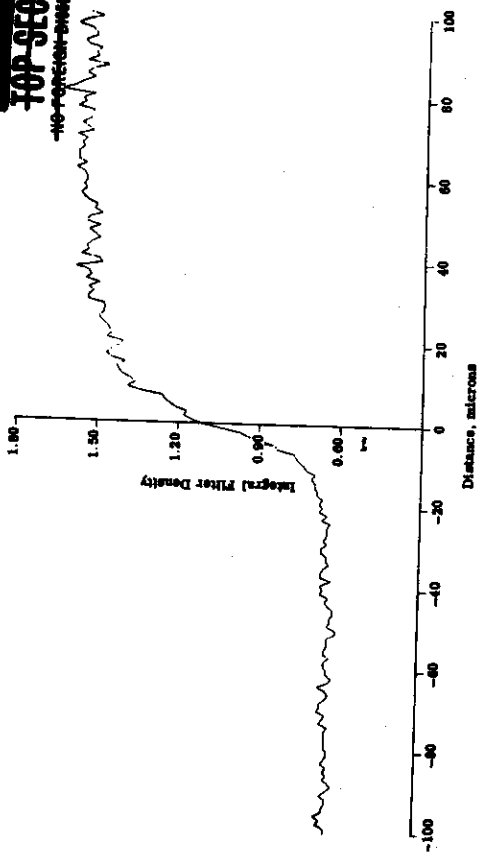
~~TOP SECRET~~
~~NO FOREIGN DISSEMINATION~~

This page intentionally blank.

~~TOP SECRET~~
~~NO FOREIGN DISSEMINATION~~

HANDLE VIA
~~TALENT KEYHOLE~~
CONTROL SYSTEM ONLY

TOP SECRET
NO FORN DISSEM



(a) Integral fiber density

(b) Analytical fiber density

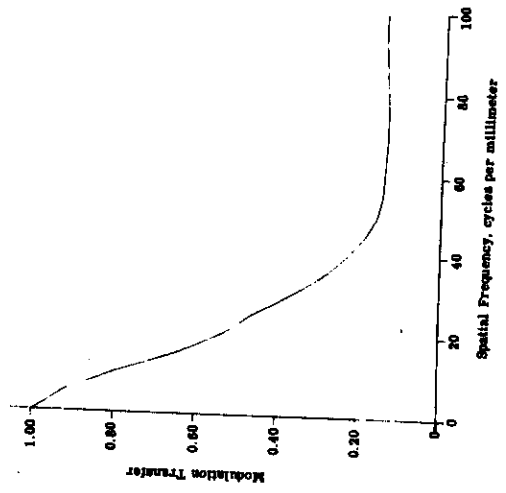
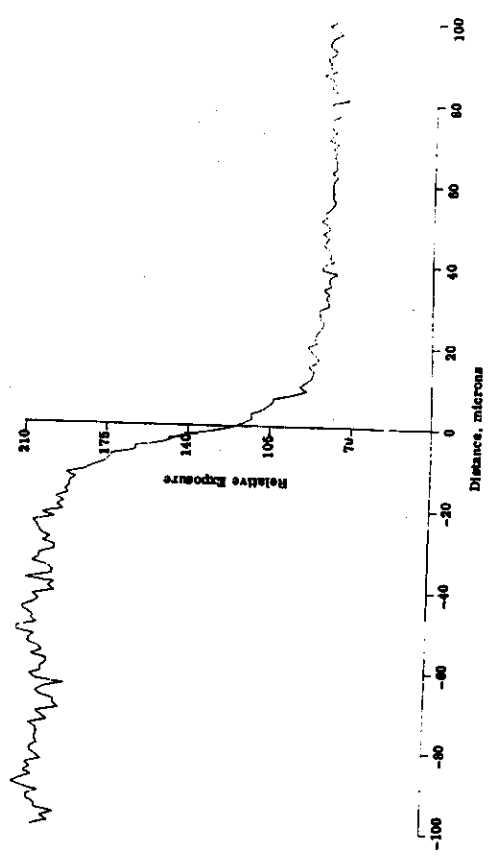
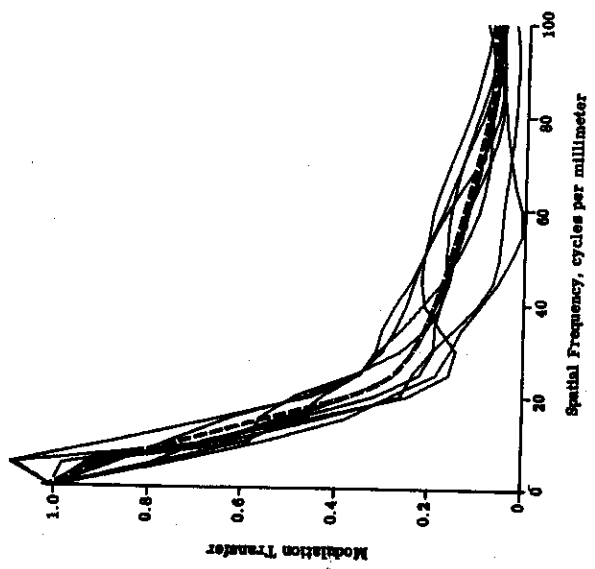


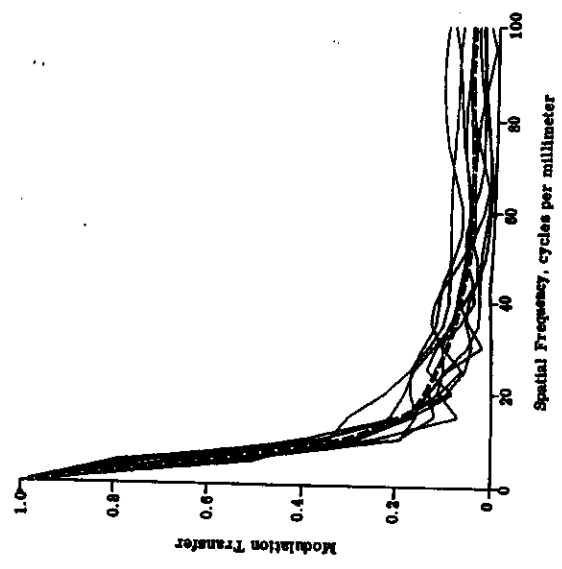
Fig. 4-8 — Illustration of steps involved in producing an MTF from a single edge trace for the cyan dye layer of SO-242 film imaged with a third generation Petval lens

HANDLE VIA

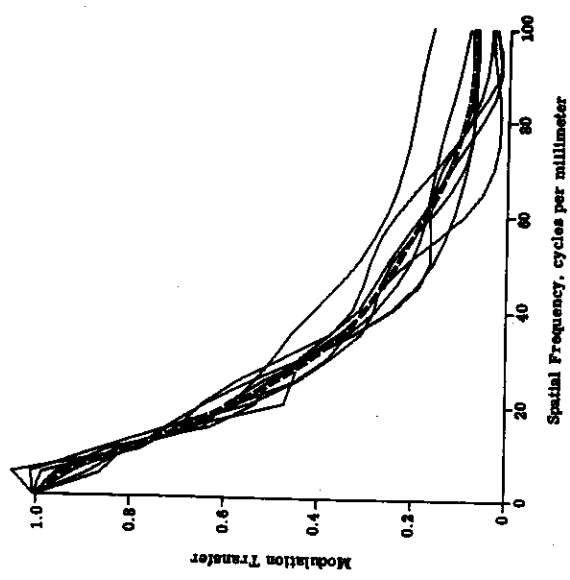
TOP SECRET



(a) Second generation Petral/SO-242 magenta dye layer

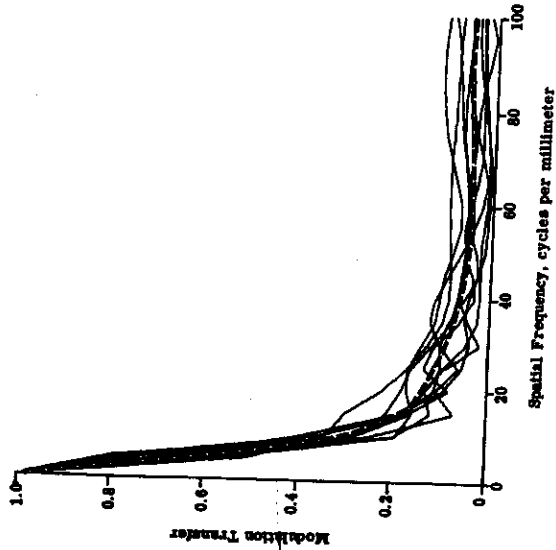


(b) Third generation Petral/SO-242 magenta dye layer

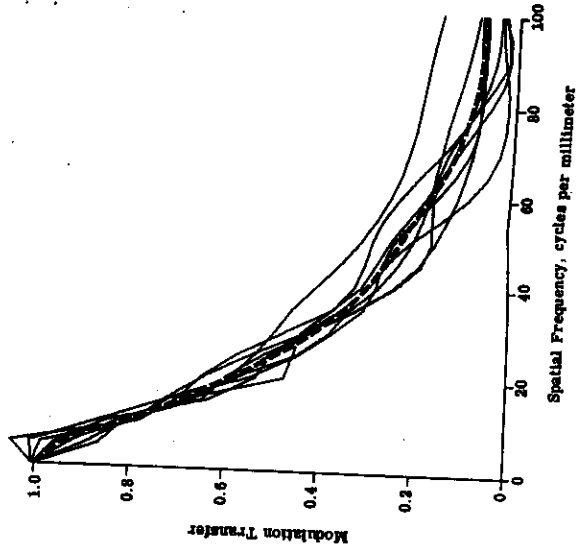


(c) Second generation Petral/SO-242 cyan dye layer

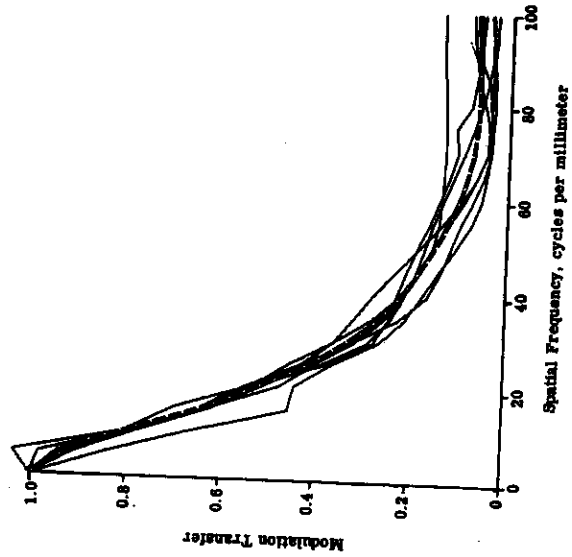
Fig. 4-9 — Lens/film MTF's determined from edge traces



(b) Third generation Petval/80-242 magenta dye layer



(c) Second generation Petval/80-242 cyan dye layer



(d) Third generation Petval/80-242 cyan dye layer

Fig. 4-9 — Lens/film MTF's determined from edge traces